

## Tunneling through highly transparent symmetric double barriers

Y. Glazer and M. Gitterman

Department of Physics, Bar-Ilan University, Ramat-Gan, 52100 Israel

(Received 27 September 1990)

We consider the tunneling through double barriers with different heights for the outer and inner edges. This difference affects the transmission coefficient, which under some conditions has non-Lorentzian behavior (absence of resonant tunneling), showing monotonic changes and a very weak dependence on energy.

The transmission of particles through a potential barrier represents one of the classical quantum-mechanical problems. Detailed physical explanations and calculations can be found, for example, in Ref. 1. Here we have restricted the discussion to the simple case of a one-dimensional system of two equal rectangular potential barriers shown in Fig. 1. Although the potential configuration in Fig. 1(a) does not have a bound state, it has a quasibound state  $E_0$  in the sense that the appropriate potential-well shown in Fig. 1(b) has the real bound state  $E_0$ . The interesting phenomenon of resonant tunneling occurs when the energy  $E$  of the incident particles from the left or from the right of the barrier of Fig. 1(a) is close to  $E_0$ . The transmission coefficient for the incident particles then becomes nearly unity even though each of the barriers has a low transparency. The theoretical explanation of this phenomenon is well known.<sup>1-4</sup> However, as described in Ref. 3, the experimental results are much weaker and less pronounced than expected from the theory. A few possible explanations for this disagreement are given in Ref. 3.

In this paper, we consider two highly transparent barriers, i.e., we assume that they are narrow (small  $d=b-a$ ) and/or low (small  $V_2$ ). It is precisely the dimensionless quantity  $d\sqrt{V_2}$  that will be treated as a small

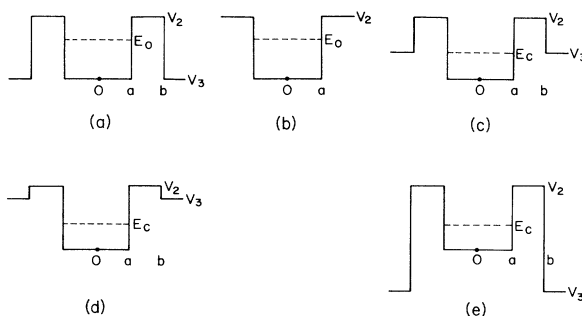


FIG. 1. Schematic representation of the rectangular potential double barriers for different outer edges  $V_3$ : (a) Typical form of the barrier of width  $d=b-a$  and height  $V_2$ ;  $E_0$  is the quasibound state,  $V_3=0$ ; (b) the potential-well equivalent to (a);  $E_0$  is the single bound state,  $V_3=V_2$ ; (c) the symmetric double barrier with the edge  $V_3$  located at  $E_c$  which divides the potential configurations with (for  $V_3 > E_c$ ) and without (for  $V_3 < E_c$ ) a bound state; (d) the double barrier with a shallow edge  $V_3$ ; (e) the double barrier with a deep edge  $V_3$ .

parameter in our analysis. (Our results will be expressed in terms of dimensionless variables. Therefore, for simplicity, we choose  $\hbar=1$  and  $m=\frac{1}{2}$  so that the energy has the dimensions of the square of the wave vector.)

The highly transparent barriers may have a bearing on the experiments described in Refs. 2-4, and they are also interesting by themselves. Indeed, we show here that nontrivial changes in the transmission coefficient occur with a change in the barrier edge  $V_3$ .

For  $V_3=V_2$  [Fig. 1(b)] and  $V_3$  close to  $V_2$  [Fig. 1(d)], a real bound state exists, whereas for  $V_3=0$  [Fig. 1(a)] or  $V_3 < 0$  [Fig. 1(e)] it is replaced by the quasibound state. The transition between these two different types of behavior occurs at some  $V_3=E_c$  [Fig. 1(c)]. One can expect, therefore, a different form for the transmission coefficient  $T$  for barriers with  $V_3 < E_c$  and for those with  $V_3 > E_c$ . In the former case, as a function of the energy  $E$  of the incident particles,  $T$  has a Lorentzian form with its maximum shifted when  $V_3$  is changed from negative values [Fig. 1(e)] through zero [Fig. 1(a)] to  $E_c$  [Fig. 1(c)]. As we will show, these maxima are located between  $E_c$  and another characteristic energy  $E_R$  such that  $E_c < E_0 < E_R$ . Moreover, in spite of an existence of the quasibound state  $E_0$ , no resonant tunneling will occur if  $V_3 < 0$  and  $E_R > V_2$ . Also, the widths of the Lorentzian curves change nonmonotonically with  $V_3$  being very small in both limiting cases,  $V_3 < 0$  and  $V_3 \leq E_c$ , reaching maximum when the peak is located near  $E_0$ .

On the other hand, for  $V_3 > E_c$ , there are no characteristic energies in the problem, and one expects monotonic behavior for  $T(E)$  for all allowed energies  $E > V_3$ . The real bound state exists for  $V_3 > E_c$  which is located deep inside the potential well and does not influence the monotonic behavior of  $T(E)$ . However, this bound state does partially trap the incident particles, thereby decreasing the transmission coefficient to less than unity.

The transition from the Lorentzian form of  $T(E)$  to monotonic behavior as  $V_3$  passes  $E_c$  must go through a series of maxima and minima which we consider here in detail. In fact, the maxima in question constitute a geometric necessity.

Note that this nontrivial behavior of  $T(E)$  is important only for highly transparent barriers, for which  $d\sqrt{V_2} \sim 1$ . When the  $d\sqrt{V_2} \gg 1$ , the energies  $E_0$ ,  $E_c$ , and  $E_R$  practically coincide, and these phenomena probably cannot be observed.

The potential-well shown in Fig. 1(b) always has, at

least, one bound state. We choose  $V_2$  and  $a$  such that only a single bound state  $E_0$  exists. This level is defined by the following transcendental equation:<sup>1</sup>

$$\tan(a\sqrt{E_0}) = \left( \frac{V_2}{E_0} - 1 \right)^{1/2}. \quad (1)$$

$$\tan(a\sqrt{E_1}) = \left( \frac{V_2}{E_1} - 1 \right)^{1/2} \{ [\sqrt{V_2 - E_1} \sinh(d\sqrt{V_2 - E_1}) + \sqrt{V_3 - E_1} \cosh(d\sqrt{V_2 - E_1})] / [\sqrt{V_2 - E_1} \cosh(d\sqrt{V_2 - E_1}) + \sqrt{V_3 - E_1} \sinh(d\sqrt{V_2 - E_1})] \}. \quad (2)$$

For  $V_3 = V_2$  the potential barrier in Fig. 1(d) reduces to that of Fig. 1(b) and, respectively, Eq. (2) reduces to Eq. (1). On the other hand, the bound-state disappears as  $V_3$  approaches  $E_c$ . One can see from Eq. (2) that the critical value of  $V_3$  (equal to  $E_c$ ), separating the configurations which have the bound state ( $V_3 > E_c$ ) from those which do not have such states ( $V_3 < E_c$ ), is defined by

$$\tan(a\sqrt{E_c}) = \left( \frac{V_2}{E_c} - 1 \right)^{1/2} \tanh(d\sqrt{V_2 - E_c}). \quad (3)$$

Another characteristic energy  $E_R$ , which defines the maximal shift of the Lorentzian peak (see below) is given by

$$\tan(a\sqrt{E_R}) = \left( \frac{V_2}{E_R} - 1 \right)^{1/2} \operatorname{coth}(d\sqrt{V_2 - E_R}). \quad (4)$$

One can ask what the connection is between the characteristic energy  $E_R$  and the height of the barrier  $V_2$ . It follows from Eq. (4) (see also Fig. 2) that  $E_R = V_2$  for  $(d/a)_{cr}$  defined as

$$[a\sqrt{V_2} \tan(a\sqrt{V_2})]^{-1} = (d/a)_{cr}. \quad (5)$$

As follows from Eqs. (1)-(5), the parameter  $d\sqrt{V_2}$  plays a special role. When this parameter is large, both Eqs. (3) and (4) reduce to (1), i.e.,  $E_R \approx E_c \approx E_0$ . For the case considered,  $d\sqrt{V_2} \approx 1$ , the three characteristic energies  $E_0$ ,  $E_c$ , and  $E_R$  are all different with  $E_R > E_0$

Let us consider now the shallow double barrier shown in Fig. 1(d). The existence of the bound state  $E_1$  for such a potential arrangement follows from the fact that  $V_3 > E_c$ . Solving the appropriate Schrödinger equation and matching the wave function and its derivatives at the boundaries  $a$  and  $b$  leads to

$> E_c$ . The dependence of  $E_c/E_0$  and  $E_R/E_0$  on  $d\sqrt{V_2}$  is shown in Fig. 2.

Let us consider now the global coefficients of transmission  $T$  and reflection  $R$  as functions of the energy  $E$  of the incident particles. All the barriers shown in Figs. 1(a), 1(c)-1(e) are symmetric about the origin. Consequently, the appropriate Schrödinger equation is invariant under space reflection and time reversal. These properties can be exploited to derive the following general form for the transfer matrix linking the incident particles with the transmitted particles:<sup>1</sup>

$$M = \begin{pmatrix} \mu + i\lambda & i\gamma \\ -i\gamma & \mu - i\lambda \end{pmatrix}, \quad (6)$$

where the real functions  $\mu, \lambda, \gamma$  are subject to the additional constraint:  $\mu^2 + \lambda^2 = 1 + \gamma^2$ .

The transfer matrix (6) determines both the transmission and reflection coefficients:

$$T = \frac{1}{\mu^2 + \lambda^2} = \frac{1}{1 + \gamma^2}; \quad R = \frac{\gamma^2}{1 + \gamma^2}. \quad (7)$$

Hence, the single function  $\gamma(E)$  determines the transmission and reflection properties of symmetric barriers. After some tedious but straightforward calculations, one obtains

$$\gamma(E) = \frac{1}{\alpha} A(E) + \alpha B(E), \quad (8)$$

where

$$A(E) = [\sinh(K_2 d) \cos(a\sqrt{E}) + \beta^{-1} \sin(a\sqrt{E}) \cosh(K_2 d)] [\beta \sinh(K_2 d) \sin(a\sqrt{E}) - \cosh(K_2 d) \cos(a\sqrt{E})], \quad (9)$$

$$B(E) = [\sinh(K_2 d) \sin(a\sqrt{E}) + \beta^{-1} \cosh(K_2 d) \cos(a\sqrt{E})] [\beta \cosh(K_2 d) \sin(a\sqrt{E}) - \sinh(K_2 d) \cos(a\sqrt{E})],$$

and

$$\alpha \equiv \frac{K_2}{K_3} = \left( \frac{V_2 - E}{E - V_3} \right)^{1/2}; \quad \beta \equiv \frac{\sqrt{E}}{K_2} = \left( \frac{E}{V_2 - E} \right)^{1/2}. \quad (10)$$

Comparing Eqs. (9) and (10) with Eqs. (3) and (4), one concludes that the zero of  $A(E)$  is located at  $E = E_R$  and that of  $B(E)$  at  $E = E_c$ . Hence for the large negative  $V_3$  shown in Fig. 1(e), when  $\alpha < 1$  the transmission

coefficient  $T(E)$  has a Lorentzian form with the maximum at  $E_R$  and whose width is determined by  $(dA/dE)_{E=E_R}$ . In the opposite limiting case of the very shallow barrier  $V_3 \lesssim E_c$  [Fig. 1(b)],  $\alpha > 1$  and the transmission coefficient again has a Lorentzian form with the maximum at  $E_c$  and whose width is proportional to  $(dB/dE)_{E=E_c}$ . It turns out that the width of the Lorentzian peak changes nonmonotonically between these two limiting cases, reaching a maximum when  $V_3 \approx 2E_0 - V_2$ , i.e.,  $\alpha \approx 1$ . For  $V_3 > E_R$  both  $A(E)$  and  $B(E)$  do

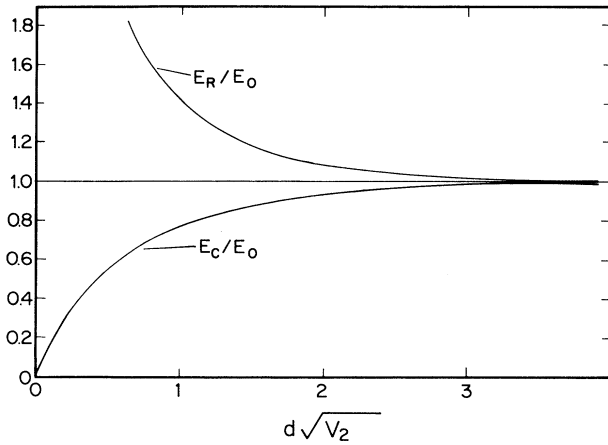


FIG. 2. Ratios of two characteristic energies  $E_C/E_0$  and  $E_R/E_0$  as a function of the parameter  $d\sqrt{V_2}$  which determines the height and the width of a barrier.

not vanish and therefore  $\gamma(E)$  and  $T(E)$  are monotonic functions of  $E$ .

Another interesting feature occurs when the width of the barriers  $d/a < (d/a)_{cr}$ , as defined by Eq. (5). When this occurs,  $E_R$  leaves the barrier,  $E_R > V_2$ , and then for  $V_3 < 0$ , the barrier becomes less penetrable. That is, no resonant tunneling takes place for such barriers in spite of the existence of a quasibound state  $E_0$ .

Let us now consider in more detail the change of  $\gamma(E)$ , and hence of the transmission coefficient  $T(E)$ , for different values of  $V_3$ . One can rewrite Eq. (8) in dimensionless form by introducing the dimensionless energy  $\epsilon = E/V_2$ :

$$\gamma = \gamma(\epsilon; a\sqrt{V_2}, d\sqrt{V_2}, V_3/V_2). \quad (11)$$

Three dimensionless parameters enter Eq. (11). These

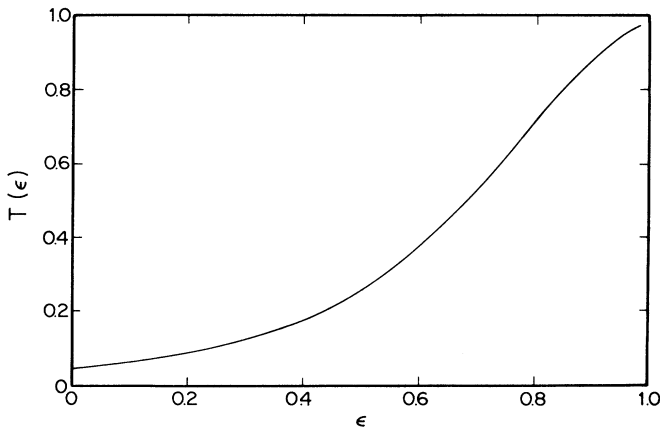


FIG. 3. Transmission coefficient  $T(\epsilon)$  as a function of the dimensionless energy  $\epsilon = E/V_2$  for a more transparent barrier than those shown in Figs. 4 and 5. Here,  $a\sqrt{V_2}$  is still equal to 1 but  $d\sqrt{V_2} = 0.5$  (i.e.,  $d/2a = 0.25$ ) and  $V_3/V_2 = -2$ . The transparency of the barrier becomes low, although the conditions for the resonant tunneling are satisfied.

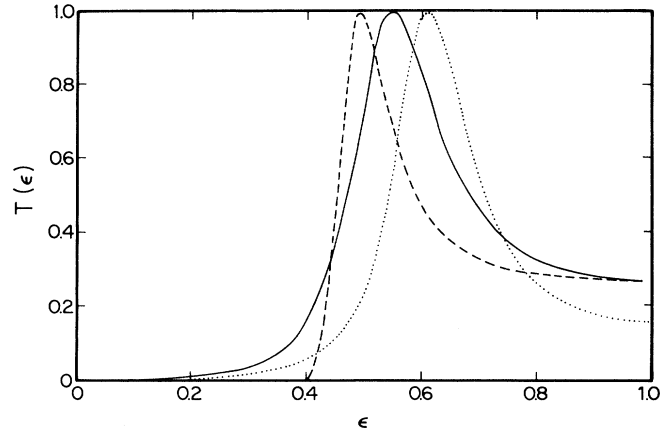


FIG. 4. Transmission coefficient  $T(\epsilon)$  as a function of the dimensionless energy  $\epsilon = E/V_2$  for  $V_3 < E_C$  (the resonant tunneling). The maximum of a Lorentzian peak is shifted with  $V_3$  while the widths are changed nonmonotonically. The parameters used are  $a\sqrt{V_2} = 1$ ,  $d\sqrt{V_2} = 1.5$  (i.e.,  $d/2a = 0.75$ ), and  $V_3/V_2 = -2, 0$ , and  $0.4$  for curves 1, 2, and 3, shown by dotted, solid, and dashed lines, respectively.

define the form of the well shown in Fig. 1(b), ( $a\sqrt{V_2}$ ); the transparency of a barrier ( $d\sqrt{V_2}$ ); and the form of the barrier edge ( $V_3/V_2$ ).

Let us now examine the transmission coefficient  $T$  as a function of the dimensionless energy  $\epsilon = E/V_2$  for different edges  $V_3/V_2$  of the double barriers for fixed values of the parameters  $a\sqrt{V_2}$  and  $d\sqrt{V_2}$ . As noted above, we assume that the potential well in Fig. 1(b) contains a single bound state which requires<sup>1</sup>  $a\sqrt{V_2} < \pi/2$ . We choose  $a\sqrt{V_2} = 1$ , and later we shall emphasize the changes resulting from

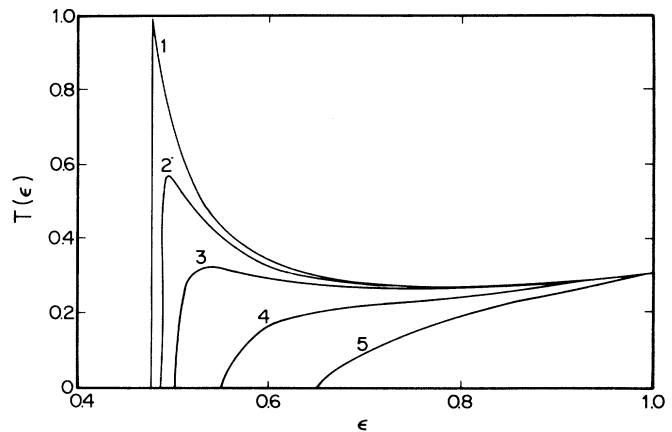


FIG. 5. Transmission coefficient  $T(\epsilon)$  as a function of the dimensionless energy  $\epsilon = E/V_2$  for  $V_3 \gtrsim E_C$ . The parameters  $a\sqrt{V_2}$  and  $d\sqrt{V_2}$  are the same as in Fig. 4, whereas  $V_3/V_2$  is larger and is assigned the values 0.477, 0.485, 0.500, 0.550, and 0.650 for the five curves 1–5, respectively. Curve 1 corresponds to  $V_3 = E_C$  and still shows resonant tunneling. Curves 4 and 5 manifest the monotonic change of  $T(\epsilon)$ , while curves 2 and 3 fall in the transition region.

larger values of this parameter. For the second parameter  $d\sqrt{V_2}$ , we choose  $d\sqrt{V_2}=1.5$ , which corresponds to the value 0.75 for the ratio of the width of the barrier and the well,  $d/2a=0.75$ . This corresponds to an experimentally achievable value which, according to Fig. 2, shows an appreciable effect. Note that in Fig. 3, we consider another value  $d\sqrt{V_2}=0.5$  (with  $d/2a=0.25$ ) which is smaller than that of Eq. (5) and hence gives no transparency at all.

For the chosen parameters  $a\sqrt{V_2}=1$  and  $d\sqrt{V_2}=1.5$ , one can easily calculate from Eqs. (1)-(4) the three dimensionless energies  $\epsilon_c \equiv E_c/V_2=0.478$ ,  $\epsilon_0 = E_0/V_2=0.546$ , and  $\epsilon_R = E_R/V_2=0.646$ .

Figure 4 shows the graph of  $T(\epsilon)$  for three different values of  $V_3/V_2$ : a negative value  $V_3/V_2=-2$  corresponding to the barrier shown in Fig. 1(e) the usual case  $V_3=0$  [compare Fig. 1(a)], and the positive value  $V_3/V_2=0.4$  which is smaller than  $\epsilon_c$ . In all these cases,  $T(\epsilon)$  reaches its maximum value of unity (resonant tunneling) at  $\epsilon=\epsilon_R$  for negative  $V_3/V_2$  and at  $\epsilon=\epsilon_0$  for  $V_3 \approx 2E_0 - V_2$  which corresponds to  $V_3 \approx 0$  for the chosen parameters.

The drastic changes occur when  $V_3$  reaches the critical value  $E_c$  [the corresponding barrier is shown in Fig. 1(c)]. The entire range of the transition from Lorentzian to monotonic behavior for  $T(\epsilon)$  is shown in Fig. 5 for  $V_3 \gtrsim E_c$ . For  $V_3=E_c$ , the function  $T(\epsilon)$  still has a maximum equal to unity on the left boundary of the energies available defined by  $V_3/V_2$ . Then, for slightly larger values of  $V_3$ , the maxima decrease drastically in height accompanied by smooth minima. Finally, at about

$V_3/V_2 \approx 0.55$ , the function  $T(\epsilon)$  becomes monotonic. The graphs in Fig. 5 begin at the threshold energy  $E=V_3$ . It can be shown from Eqs. (7)-(9) that the dependence of  $T(\epsilon)$  near that threshold is linear.

A very special case is depicted in Fig. 3. This graph corresponds to the negative  $V_3/V_2=-2$  and to  $d\sqrt{V_2}=0.5$  which, according to Fig. 2, corresponds to  $E_R > V_2$ . No resonant tunneling occurs under these conditions and  $T(\epsilon)$  is again monotonic and small, even though resonant tunneling is expected.

The above-mentioned nontrivial behavior of  $T(\epsilon)$  exists not only for our choice of parameters. More than one bound state exists for the potential well shown in Fig. 1(b) for  $a\sqrt{V_2} > \pi/2$ . Here, too, the transition to monotonic behavior occurs for resonant tunneling on each of the quasibound states. In other words, the graphs in Fig. 4 will now have several maxima, and each of them will disappear as shown in Fig. 5. More serious is the following restriction on the parameter  $d\sqrt{V_2}$ . This parameter is restricted from above (barriers have to be highly transparent) to make sure that  $E_c$ ,  $E_0$ , and  $E_R$  [given by Eqs. (1)-(4)] are practically indistinguishable.

We look forward to experimental verification of these predictions by measuring the current-voltage characteristics of semiconductor quantum wells created, for example, by layers of  $\text{Al}_x\text{Ga}_{1-x}\text{As}$ . For a quantitative comparison with experiment, some modifications to our simplified model have to be introduced.

It is a pleasure to acknowledge very useful discussions with M. Azbel, R. Berkovitz, and L. Horovitz.

<sup>1</sup>E. Merzbacher, *Quantum Mechanics* (Wiley, New York, 1986).

<sup>2</sup>E. O. Kane, in *Tunneling Phenomena in Solids*, edited by E. Burstein and D. Lundquist (Plenum, New York, 1969), pp.

1-11.

<sup>3</sup>B. Ricco and M. Ya. Azbel, *Phys. Rev. B* **29**, 1970 (1983).

<sup>4</sup>A. S. Davydov and V. N. Ermakov, *Physica D* **28**, 168 (1987).